Available online at www.sciencedirect.com
ScienceDirect
Journal of the European Ceramic Society 29 (2009) 3185–3195
www.elsevier.com/locate/jeurceramsoc

Influence of the urea content on the YSZ hydrothermal synthesis under dilute conditions and its role as dispersant agent in the post-reaction medium

I. Gonzalo-Juan, B. Ferrari, M.T. Colomer *

Instituto de Cerámica y Vidrio, CSIC, c/Kelsen, 5, Cantoblanco 28049, Madrid, Spain

Received 25 November 2008; received in revised form 13 April 2009; accepted 22 April 2009
Available online 8 July 2009

Abstract

The effect of the urea content, under mild and dilute conditions, on the extension of the YSZ hydrothermal reaction, on the crystalline zirconia phases obtained and, on its primary particle size has been studied. The key role of the urea as a dispersant agent for the synthesized YSZ nanoparticles has also been investigated in terms of particle size distribution and zeta potential. The latest study has been performed in the post-reaction medium. Pure nanocrystalline YSZ is obtained when a basic pH (∼10) is achieved during the synthesis. In addition, the urea is protonated at $5 < pH < 7$ in the post-reaction medium and it allows its specific adsorption on the surface of the particles by electrostatic and steric mechanisms, keeping a stable suspension. In those conditions, the measured average particle size is 20 nm and the agglomeration factor (F_{ag}) is 2. However, by HR-TEM particles with a size even less than 5 nm are observed.

Keywords: Powders-chemical preparation; Suspensions; ZrO_2; Fuel cells

1. Introduction

Yttria stabilized zirconia (YSZ) is an important ceramic material for functional and structural applications such as catalyst support, oxygen sensor, electrochemical oxygen pump, thermal barrier coating, solid electrolyte in solid oxide fuel cells (SOFCs), etc.[1–5] To improve the sinterability of YSZ and thus their properties is necessary to obtain pure and weakly agglomerated nanocrystalline powders. Taking into account this purpose, different physical, mechanical and chemical methods of synthesis have been researched. YSZ powders are routinely synthesized by conventional solid-state reactions at such high temperatures in which particles sinter, loosing their fine particulate nature. Wet synthesis methods as co-precipitation, sol–gel, microemulsions or hydrothermal techniques have been investigated to overcome this problem with different degrees of success.[1,6,7] Among wet-chemical methods, hydrothermal synthesis can be considered the best alternative because it is an ecological soft chemical route, using low work temperatures and obtaining nanometer sized crystalline powders with weakly bonded agglomerates.[8] Hydrothermal synthesis of YSZ involves an initial co-precipitation followed by a higher temperature hydrothermal treatment to obtain the anhydrous crystalline powder,[9] being the calcination process not necessary.[6] The hydrothermal synthesis can be carried out by two different routes depending on whether the temperature and pressure of the water are sub-critical or supercritical ($T_c = 374\,^{\circ}C$, $P_c = 22.1$ MPa).[10,11] When the hydrothermal process is performed under sub-critical conditions, it is necessary to use a reactant which forces the co-precipitation of the metal hydroxides in a relatively short time.[12] This kind of hydrothermal synthesis can be carried out under strong or mild conditions depending on the pH modification that can occur when these reactants are added to the reaction mixture. There are several reports in the literature on the hydrothermal synthesis of different metal oxide-doped zirconia powders in basic solution under diverse conditions of temperature, time and precursors in order to obtain the cubic phase. The most common reagents used to achieve the strong conditions are alkaline hydroxides or alkaline carbonates solutions, in particular sodium or potassium are the most employed alkaline ions.[8,13–17] However, it is well known that Na_2O at a concen-

* Corresponding author.
E-mail address: tcolomer@icv.csic.es (M.T. Colomer).

0955-2219/$ – see front matter © 2009 Elsevier Ltd. All rights reserved.
doi:10.1016/j.jeurceramsoc.2009.04.041

tration level of hundreds ppm causes serious damage to zirconia electrolytes.[18]

Urea has been used frequently in many forced-hydrolysis processes for ultrafine particle synthesis.[12] It is well established that during the thermal treatment at temperatures between 80 and 100 °C, the urea in water solution is gradually decomposed to release OH^-. Some researchers have reported the hydrothermal conditions required for synthesizing nanoparticles stabilized zirconia under mild conditions.[12,19–34] For instance, the characteristics of the scandia-stabilized zirconia powders, such as, crystalline size, crystalline phase, particle size distribution, degree of agglomeration and strength of the agglomerates synthesized, are controlled by the pH at the end of the reaction, ion concentration and salts used as starting reagents, pressure, volume, temperature and time, i.e. thermal treatment.[19,20]

Xu et al.[20] studied the effect of urea and cation concentration on the amount of the monoclinic phase obtained on the hydrothermal synthesis of 8ScSZ powders and concluded that the monoclinic fraction in the as-synthesized powders increased with increasing the urea from 0.1 to 1.5 mol L^{-1} by maintaining the ratio of cations to urea equal to 1:4. In addition, the effect of the urea concentration in the crystalline size was also investigated, and was observed that dilute urea concentrations in the reaction mixture lead to complete crystallization and a big crystallite size compared to solutions with higher urea concentration (>0.8 mol L^{-1} of urea when the cation concentration was fixed at 0.05 mol L^{-1}), where full crystallization does not occur, resulting in smaller crystallite sizes. The same work also concluded that the amount of monoclinic phase increases on cation concentration from 0.05 to 0.5 mol L^{-1} by maintaining the ZrO^{2+}:urea ratio equal to 1:4. Although, different researchers have reported the hydrothermal conditions required for synthesizing nanoparticles of stabilized zirconia using urea as starting reagent,[12,19–34] concentrated conditions were always employed. In addition, the role of the urea as dispersant agent has not been studied in depth.

The aims of the present work are to study the effect of the urea content on the extension of the reaction, on the zirconia crystallization and on zirconia primary particle size under mild and dilute hydrothermal conditions. The effect of the urea on the agglomeration state of the resulting zirconia nanoparticles and their dispersion in the mother liquor, in terms of particle size distribution and zeta potential, has been also investigated. Dilute conditions were selected in this study in order to minimize the formation of monoclinic zirconia phase.[19,20]

2. Experimental

2.1. Preparation of stock solutions and synthesis

Zirconyl chloride octahydrated analytical grade ($ZrOCl_2{\cdot}8H_2O$ from Alfa Aesar, USA) was used as the zirconium source and yttrium chloride hexahydrated analytical grade ($YCl_3{\cdot}6H_2O$, from Aldrich, Germany) was used as the yttrium source. Appropriate amounts of each precursor were employed to prepare the stock solutions with a cation concentration of 5×10^{-2} M (ZrO^{2+} ion) and 5×10^{-3} M ($2Y^{3+}$ ion) distilled water solutions at room temperature. A 8×10^{-2} M solution of urea (Panreac, Spain) was also employed as starting reagent.

The stock solutions of the metal chlorides and urea were mixed at room temperature in the adequate proportions. The molar ratios of the ZrO^{2+}:urea employed were 1:1 (stoichiometry) and 1:2.2 (superstoichiometry). A hydrothermal synthesis with no urea addition was also carried out. In addition, two different thermal treatments have been employed in order to establish the extent of the reaction at every step. The first thermal treatment (I) consisted in a single-step program run at 180 °C for 48 h and the second one (II) was a two-step program run with a previous stage at 80 °C for 24 h and a second one at 180 °C for 48 h (I). Table 1 summarizes the concentrations of each precursor and the urea solutions and the thermal treatment used in each synthesis. A 300 mL stainless-steel reactor with Teflon inner container was filled up with each solution up to 86 vol.% of its capacity. If the product was a powder when the process finished, it was filtered and dried at 60 °C for 2 h. Thermal treatments and powders drying were carried out in air in an automatic program heater (Binder, Germany).

2.2. Morphological, textural, thermal and crystallographic characterization methods

The morphology and microstructure of the obtained powders and dried sols were observed by using transmission electron microscopy (TEM), and selected area electron diffraction (SAED), if they were sols. The powders were suspended in the mother liquor by stirring. The as-prepared samples (sols and suspensions) were dropped on a copper grid, and then allowed to dry under a heat lamp. The observations were carried out on a microscope working at 125 keV (Hitachi H7100, Japan) and on a field emission electron microscope working at 200 keV (High resolution transmission microscopy (HR-TEM) JEM-2100F JEOL, Japan). Local composition was analyzed by energy dispersive of X-ray (EDX) with an ISIS analyzer system attached to the above mentioned microscope.

Differential thermal analysis and thermogravimetry (DTA-TGA) of dried powders was carried out in air (DTA-TGA-7, PerkinElmer, USA) at a heating rate of 10 °C/min up to 1000 °C. Phase identification of the as-prepared and calcined powders was carried out by X-ray diffraction, with a diffractometer (D5000, Siemens, Germany) using a Cu Kα radiation collected at room temperature over a range of $20° \leq 2\theta \leq 80°$ at a step scan rate of 2°/s. Furthermore, phase identification was also performed by FT-Raman (Renishaw, United Kingdom). The excitation source employed was a Nd-YAG laser, emitting at a frequency of 514.5 nm line as the excitation source. A laser power of 25 mW was used, and was collected over an effective spectral range of 700–100 cm^{-1}.

The specific surface area (SSA) was measured by N_2 adsorption–desorption, BET method (Monosorb Surface Area Analyzer MS-13, Quantachrome Co., USA), and the density (ρ) of the powders was measured by helium pycnometry (Multipycnometer, Quantachrome Co., USA). The errors of those techniques are ±5% and ±10%, respectively.

Table 1
Hydrothermal synthesis conditions used: starting reagents and their concentrations, ZrO^{2+}:urea molar ratio and thermal treatment employed.

Synthesis	$ZrOCl_2{\cdot}8H_2O$ (mol/L)	$YCl_3{\cdot}8H_2O$ (mol/L)	Urea (mol/L)	ZrO^{2+}:urea molar ratio	Thermal treatment
HS_I	4×10^{-3}	3.2×10^{-4}	0	1:0 (without urea)	I
HS_{II}	4×10^{-3}	3.2×10^{-4}	0	1:0 (without urea)	II
$HS_{II,st}$	4×10^{-3}	3.2×10^{-4}	4×10^{-3}	1:1 (stoichiometry)	II
$HS_{I,sup}$	4×10^{-3}	3.2×10^{-4}	8.8×10^{-3}	1:2.2 (superstoichiometry)	I
$HS_{II,sup}$	4×10^{-3}	3.2×10^{-4}	8.8×10^{-3}	1:2.2 (superstoichiometry)	II

2.3. Suspension characterization methods

The pH and the concentration of Y^{3+} and Zr^{4+} cations dissolved in the mother liquor after the hydrothermal reaction were determined. The pH was measured by a pH-meter (691 pHmeter, ΩMetrohm, Switzerland). The cation concentration was determined by inductively coupled plasma-atomic emission spectrometry technique (ICP-AES) (Thermo Jarrell ASH, Irish Advantage Duo, USA). The error associated to this technique is about ±2%.

The particle size distribution and the zeta potential of nanoparticles were determined by dynamic light scattering (DLS) and laser Doppler velocimetry, respectively (Zetasizer Nano ZS, Malvern S, UK). If the powder is assumed to be monodispersed and spherical, an average particle diameter, having the same surface than the powder under investigation (in m^2/g), can be calculated. This is normally written as d_{BET} and is obtained using the adsorption model from the nitrogen adsorption isotherm.[35] In addition, the d_v50/d_{BET} ratio can be defined as the agglomeration factor, F_{ag}, being indicative of the state of agglomeration of the powder in the suspension.[36]

The particle size of the suspensions was characterized immediately after their synthesis. The powders were suspended in the mother liquor by stirring for 1 h. Suspensions were then diluted before measuring with distilled water (if necessary). The sonication effect (Ultrasonication Probe, UP 400S, Hielscher, Germany) was study as dispersant method to determine the agglomerate strength. The suspensions were diluted up to a solids concentration of $\sim10^{-3}$ g/L, with a 10^{-2} M KCl solution, to perform the zeta potential measurements. To fit the pH of the suspensions to acidic or basic conditions HCl and KOH electrolytes were used, respectively.

To study the effect of urea as dispersant agent on the particle stability the addition of this reagent after the synthesis was also considered. Urea amounts of up to 2 wt.% related to the solids content were added to the suspension obtained after the $HS_{II,st}$ synthesis. An urea amount similar to those needed to achieve a molar ratio ZrO^{2+}:urea equal to 1:2.2, i.e. ∼67 wt.%, was also considered for comparative purposes and added to the suspension obtained from the $HS_{II,st}$ synthesis. The resulting suspension is labeled $HS_{II,st}$ + U. The particle size distribution after sonication was measured for all the urea concentrations. The zeta potential were also determined vs. urea addition for the as-prepared $HS_{II,st}$ suspension.

3. Results and discussion

3.1. Influence of the urea content on the synthesis reaction and the resulting products

As is mentioned above, dilute solutions of the reagents (Table 1) were considered for this study. Different syntheses were performed with and without urea addition. In this sense, two urea contents as reagent were considered: the first one with a stoichiometric urea amount and the second one with an amount in excess, in both cases related to the ZrO^{2+} concentration (Table 1). In addition, for the extreme conditions considered (without urea and urea in excess), two thermal treatments were chosen. Both protocols differ in a low temperature dwell (80 °C for 24 h), which should insure a slow hydrolysis rate for the urea and co-precipitation of the hydroxide.[20]

After the hydrothermal process, two different products have been obtained depending on the ZrO^{2+}:urea molar ratio employed in the synthesis. If urea was not added a sol is obtained as a final product (HS_I and HS_{II} syntheses), while the resulting product was a powder when the molar ratio was equal or higher than that of the stoichiometric ratio ($HS_{II,st}$, $HS_{I,sup}$ and $HS_{II,sup}$).

Table 2 summarizes the hydrothermal synthesis conditions of this study: the thermal treatment, the ZrO^{2+}:urea ratio, the pH of the reagents solution (pH_0), and some of the characteristics of the reaction products such as, the pH of the sols/mother liquor at the end of the treatment (pH_f), the concentration of Zr^{4+} and Y^{3+}

Table 2
Hydrothermal synthesis conditions used, pH measurements before (pH_0) and after (pH_f) the hydrothermal synthesis have been finished, products obtained as a function of the ZrO^{2+}:urea molar ratio employed and [Zr^{4+}] and [Y^{3+}] ions dissolved in the $HS_{II,st}$, $HS_{I,sup}$ and $HS_{II,sup}$ mother liquors after synthesis measured by ICP-AES, specific surface area (SSA) and density (ρ) of the $HS_{II,st}$, $HS_{I,sup}$, $HS_{II,sup}$ as-prepared powders.

Synthesis	Thermal treatment	ZrO^{2+}:urea molar ratio	pH_0	pH_f	Product obtained	[Zr^{4+}] dissolved (mol%)	[Y^{3+}] dissolved (mol%)	SSA ($m^2\,g^{-1}$)	ρ ($g\,cm^{-3}$)
H_IS	I	1:0	2.0	2.3	Sol				
HS_{II}	II	1:0	2.0	3.0	Sol				
$HS_{II,\,st}$	II	1:1	2.0	3.3	Powder	<1.30 ± 0.02	30.00 ± 0.8	159 ± 3	3.87 ± 0.01
$HS_{I,\,sup}$	I	1:2.2	2.0	9.7	Powder	2.30 ± 0.04	0.10 ± 0.01	185 ± 2	3.95 ± 0.01
$HS_{II,\,sup}$	II	1:2.2	2.0	9.7	Powder	5.60 ± 0.09	0.30 ± 0.02	160 ± 3	4.11 ± 0.01

dissolved in the mother liquor of $HS_{II,st}$, $HS_{I,sup}$ and $HS_{II,sup}$, the specific surface (SSA), and the density (ρ) of the powders obtained from the three latest reactions.

The pH_f depends on the urea amount used for the synthesis as shown in Table 2. When urea was added in quantities higher than the stoichiometric one the pH_f was alkaline ($pH_f = 9.7$). However, when the quantity added was stoichiometry or when the synthesis occurs without urea the pH_f in both cases resulted acidic. These results are in accordance with the competition of the urea decomposition to release OH^- (Eq. (1))

$$CO(NH_2)_2 + 3H_2O \rightarrow CO_2 + 2NH_4{}^+ + 2OH^- \quad (pH \uparrow) \tag{1}$$

and with the hydroxylation of the zirconyl and yttrium chlorides reactions (Eqs. (2)–(4)), that is,

$$ZrOCl_2 + H_2O \rightarrow ZrO_2(s) + 2HCl \tag{2}$$
$$2YCl_3 + 3H_2O \rightarrow Y_2O_3(s) + 6HCl \tag{3}$$

$$ZrOCl_2 + 2YCl_3 + 4H_2O \rightarrow Zr(Y)O_2 + 8HCl \quad (pH \downarrow) \tag{4}$$

During the hydrothermal process, the gradual, homogeneous release of OH^- from urea balances the acidity increase due to the thermal hydroxylation/condensation of zirconyl and yttrium solution and, thus, helps the reaction progress toward yttrium-doped zirconia particle precipitation (Eqs. (2)–(4)).[22–25] In the HS_I and HS_{II} reactions, the pH is acidic at the end of the reaction (pH_f) and, a sol is attained in both cases.

However, a precipitate was obtained when urea was added, even under acidic conditions (Table 2). The resulting precipitates in $HS_{I,sup}$, $HS_{II,sup}$, and $HS_{II,st}$ syntheses were dried at 60 °C and characterized. The densities of the dried powders are lower than that of the theoretical values for the YSZ ($\rho = 6.1\ g\ cm^{-3}$),[37] but the specific surface areas ($159–185 \pm 3\ m^2\ g^{-1}$) are in the range of the reported data for nanometric particles of YSZ.[19] Moreover, the concentration of Zr^{4+} dissolved in the mother liquor at the end of the powder synthesis is lower than 6 mol%, indicating that the yields, calculated from the ICP measurements (Table 2), of all the synthesis performed with urea ($HS_{II,st}$, $HS_{I,sup}$ and $HS_{II,sup}$) are higher than 90%.

Nevertheless, it is noticed that the concentration of Y^{3+} dissolved related to the amount of urea added after the $HS_{I,sup}$, $HS_{II,sup}$ syntheses which reach basic pHs are $\leq$0.3 mol%, and 30 mol% after the $HS_{II,st}$ synthesis when the pH_f was acid. The partial dissolution of yttrium in acid media is well known for Y-TZP powders.[38] Hence, the high concentration of Y^{3+} in the mother liquor of the $SH_{II,st}$ synthesis indicates that the Y^{3+} is partially dissolved.

In order to determine the primary particle size and the extension of the HS_I and HS_{II} reactions, the as-prepared sols were dried and then characterized by TEM-EDX and Raman techniques. Fig. 1 shows the TEM micrographs of the dried powders. The SAED patterns shown as insets in both micrographs provide a direct evidence of the microstructure of the materials obtained.

Primary particle size can be estimated from the TEM micrographs, being in the order of ~10 nm. Particles have a spherical morphology and they present a high degree of agglomeration. The agglomerates formed and the primary particle size seem not to be affected by the thermal treatment. In both cases, large agglomerates higher than 100 nm can be observed (arrows in Fig. 1). Otherwise, in both cases a typical diffraction pattern of a polycrystalline sample (diffraction rings instead of well defined spots) is observed. The diffuse maxima obtained can be explained as a result of small domain size (<10 nm) together with poor crystallinity at the atomic scale.

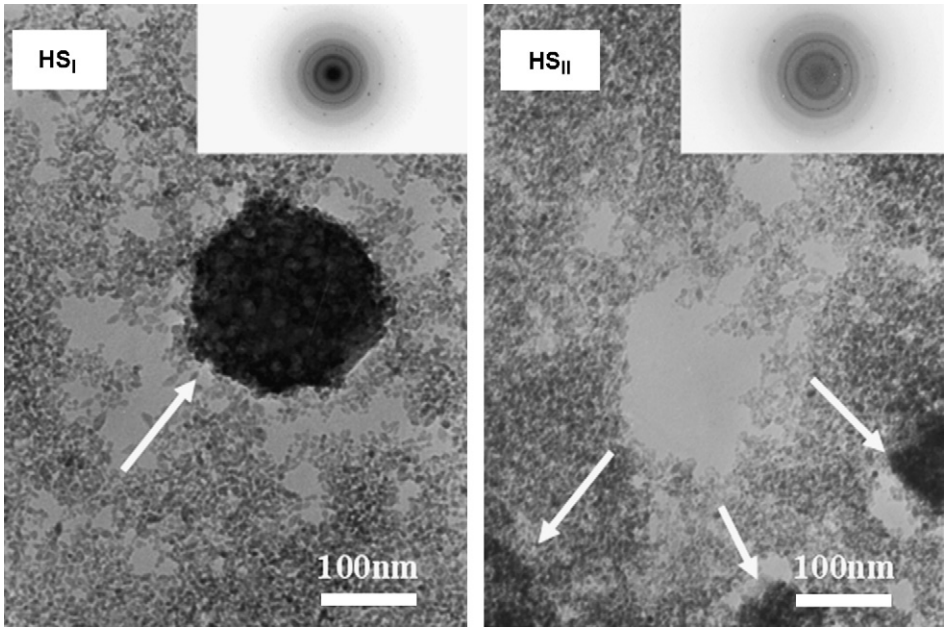

Fig. 1. TEM micrographs of the HS_I and HS_{II} powders and their corresponding SAED patterns.

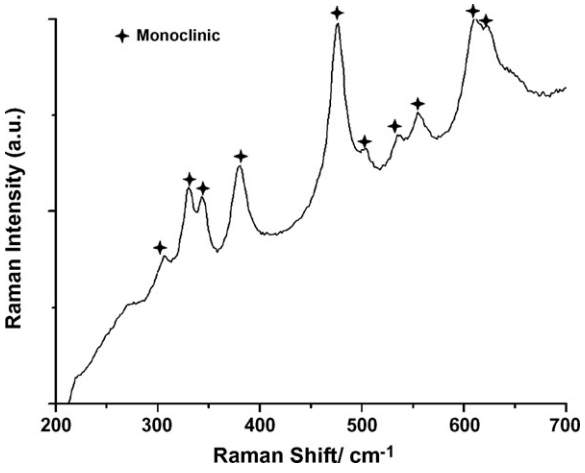

Fig. 2. Raman spectrum of the dried powder from the HS_{II} sol.

Fig. 2 shows the FT-Raman spectrum for the dried powder prepared from the HS_{II} sol. This spectrum corresponds to the monoclinic zirconia phase, neither cubic nor tetragonal phases are observed.[39] This result together with the pH measured at the end of the process, $pH_f = 2.3$, can indicate that Y^{3+} keeps dissolved during the hydrothermal process and thus yttrium hydroxylation has not been taken place at that point. Hence, the product of the hydrothermal synthesis formed without urea seems to be independent on the thermal treatment used in this study (I or II), since in any case the time considered is enough to complete the synthesis reaction. The product obtained from both synthesizes is a nanometric powder, strongly agglomerated, of monoclinic zirconia showing a poor crystallinity.

The dried powders attained in the $HS_{II,st}$, $HS_{II,sup}$, and $HS_{I,sup}$ syntheses were characterized by TEM-EDX and XRD techniques. Fig. 3 shows the TEM micrographs of the as-synthesized powders obtained by the $HS_{II,st}$ (Fig. 3a) $HS_{I,sup}$ (Fig. 3c) and $HS_{II,sup}$ (Fig. 3e) syntheses, and their corresponding XRD patterns (Fig. 3b, d and f, respectively).

Typically, agglomerates of very fine crystals (ca. lower than 10 nm) could be seen by TEM in all cases. Particles have a spherical morphology, but also form agglomerates of ~100 nm. The XRD patterns (Fig. 3b, d and f) corresponding to the as-prepared powders present very broad and weak intensity peaks due to the nano-effect indicating a small domain size.[40] These results are supported by the high specific surface area shown in Table 2 and the primary particle sizes observed by TEM.

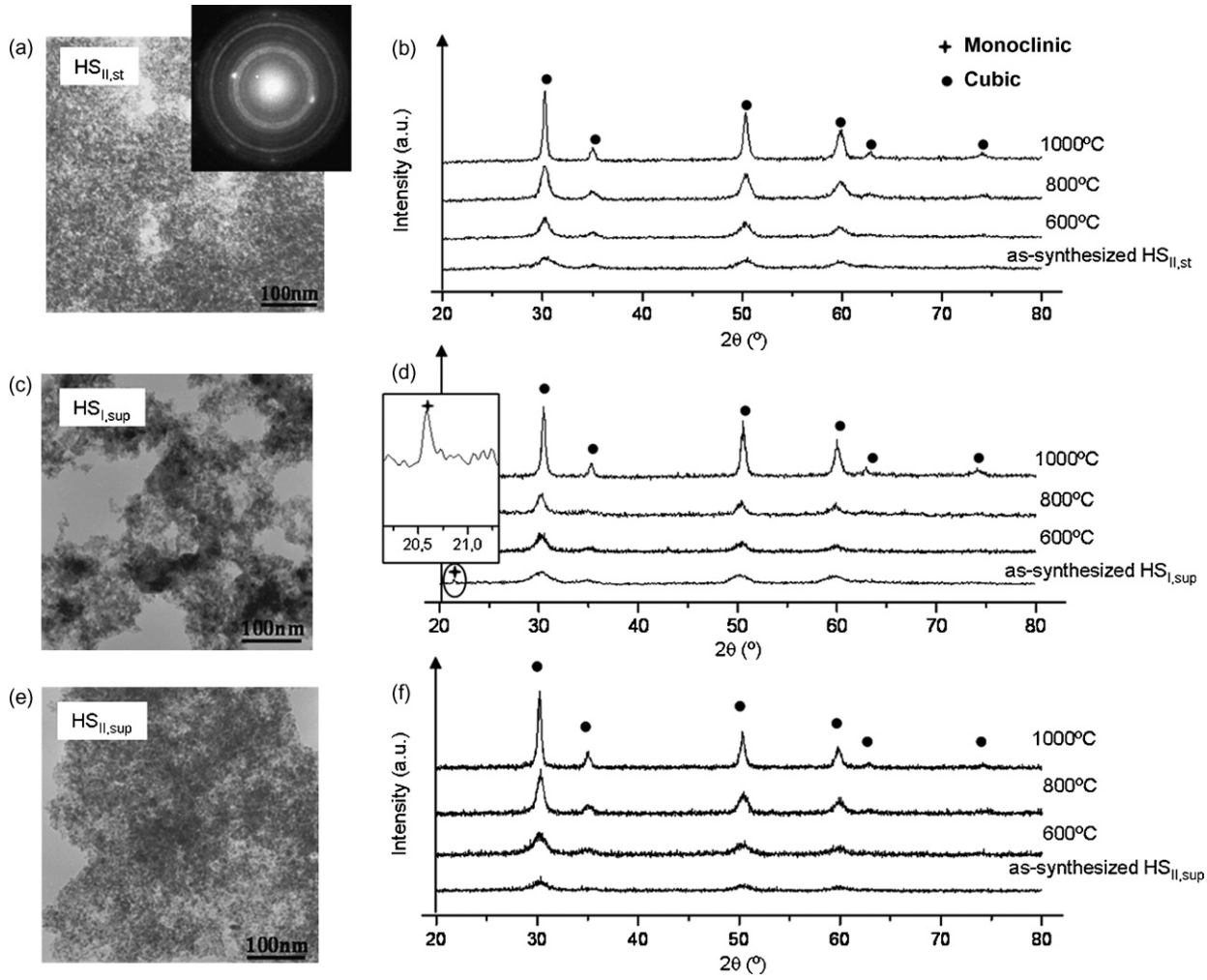

Fig. 3. (a), (c) and (d) TEM micrographs of the as-synthesized powders $HS_{II,sup}$, $HS_{I,sup}$, HS_{II} and (b), (d) and (f) their XRD patterns of the as-synthesized powders and of the powders calcined at different temperatures: 600, 800 and 1000 °C.

Comparing the TEM micrographs of the three powders obtained, those synthesized from the $SH_{II,st}$ reaction seem to be the least agglomerated ones. However, comparing the powders from syntheses performed under different thermal conditions, i.e. $HS_{I,sup}$ (Fig. 3c) and $HS_{II,sup}$ (Fig. 3e) a stronger agglomerated powder is observed when the thermal cycle used is the shortest one ($HS_{I,sup}$).

The SAED diagram, shown as inset in the micrograph for the $HS_{II,st}$ (Fig. 3a), provides well defined spots characteristic of a better ordered single crystal that those showed in Fig. 1 for the product of the SH_I and SH_{II} synthesises. The EDX microanalysis confirms the chemical homogeneity of the powders. Otherwise, it is not possible to verify whether the prepared phase is cubic and/or tetragonal, since the line broadening of the XRD patterns due to the fine crystallite size does not allow discriminate between both phases (Fig. 3b, d and f). When the as-prepared powders were calcined at different temperatures (600, 800 and 1000 °C) a higher crystallinity was observed in all of them, verifying that after a thermal treatment at 800 °C the cubic zirconia is the unique phase present in all cases.

In spite of the $HS_{I,sup}$ reaction reaches a basic pH (Table 2), the absence of the first dwell (80 °C for 24 h) in the thermal treatments leads to a strongly agglomerated powder and a fraction of monoclinic zirconia in the as-prepared powder detected by XRD (Fig. 3d). The XRD pattern of the $HS_{I,sup}$ as-synthesized powders reveals the existence of the (0 1 1) peak which corresponds to the most intense peak for the monoclinic phase ($2\theta = 20.58°$). This feature keeps for the powder calcined at 600 °C and disappears when the powder was treated at 800 °C. Consequently, when urea was added as reagent, the hydrothermal conditions must be designed to firstly promote its decomposition in order to allow a complete reaction. In this sense, the products of the synthesis $HS_{I,sup}$ have not longer characterized in this study. For the powders from the $HS_{II,st}$, $HS_{II,sup}$ syntheses is not possible to establish if the monoclinic phase is also present as a secondary phase from the XRD patterns.

Since FT-Raman spectroscopy is a more sensitive technique than XRD, the former can be employed not only for establishing the presence of the major phase but also the presence of minor phases. The spectra of the as-synthesized powders from the $HS_{II,st}$, and $HS_{II,sup}$ syntheses are depicted in Fig. 4. The characteristic band of the cubic zirconia phase at 607 cm^{-1} is observed in both samples.[41] In addition, the Raman spectra of both powders show additional peaks which can be associated to monoclinic zirconia.[41] As is mentioned above, the monoclinic phase was not detected by XRD, hence we can conclude that this phase is present under the XRD detection limit in both cases. In the case of $HS_{II,sup}$ synthesis only a 0.3 mol% of yttrium is detected in the mother liquor by ICP-AES. Thus, the monoclinic phase should be as a trace in the synthesized powder. In conclusion, the urea used for the synthesis should provide a medium pH basic enough to achieve the total hydroxylation and condensation of the zirconyl and yttrium chlorides. In addition, the use of the urea in the hydrothermal synthesis of stabilized zirconia powders, not only plays a key role in the hydrothermal process under concentrated conditions[22] but also under dilute conditions.

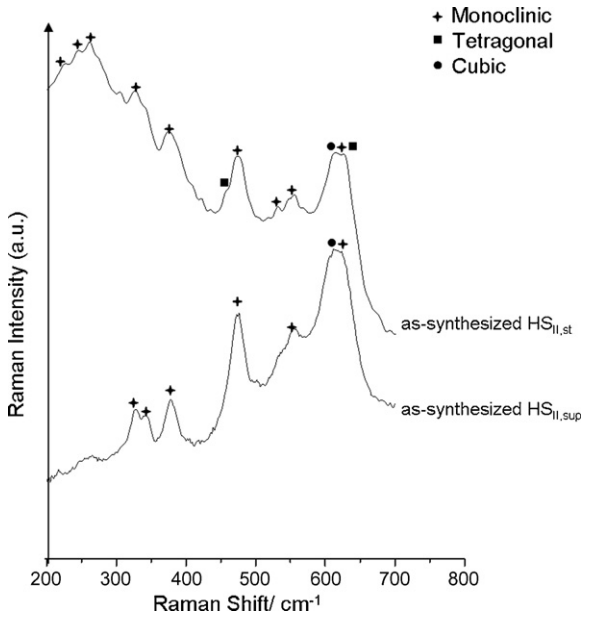

Fig. 4. Raman spectra of the as-synthesized $HS_{II,st}$ and $HS_{II,sup}$ powders.

In the spectrum for the sample $HS_{II,st}$ two bands at 475 and at 630 cm^{-1} are detected and can be related to the tetragonal zirconia phase.[40] A significant amount of yttrium dissolved in acid media (30 mol%) after the synthesis end can explain the presence of both tetragonal and monoclinic zirconia phases for the $HS_{II,st}$ synthesis. In spite of the urea decomposition at 80 °C had promoted the hydroxylation of the zirconyl and yttrium cations and then the corresponding co-precipitation, the pH achieved at the end was acidic since a part of the yttrium could return to the mother liquor from the zirconia lattice.[40]

Fig. 5 presents the thermal evolution in air of the as-prepared powder at the $HS_{II,st}$ synthesis. The resulting powder presents only the cubic phase according to the X-ray measurements and monoclinic and tetragonal phases as secondary phases according to FT-Raman results. Thus, both monoclinic and tetragonal zirconia phases are present as secondary phases.

The TG results indicate that the overall weight loss is about 50 wt.% of the sample. The first 8 wt.% loss observed below

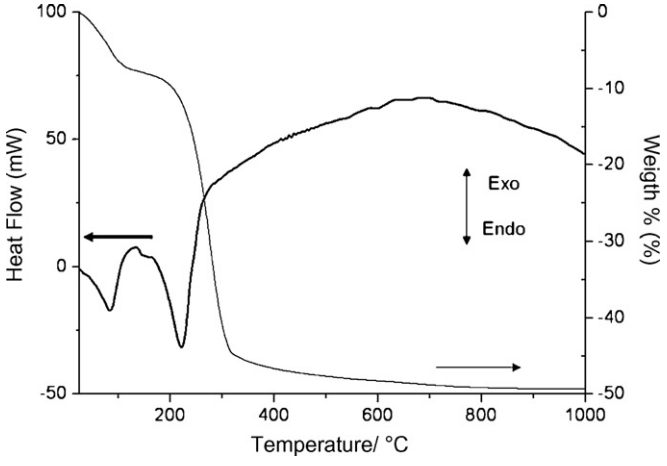

Fig. 5. DTA-TG scan curves of the sample $HS_{II,st}$.

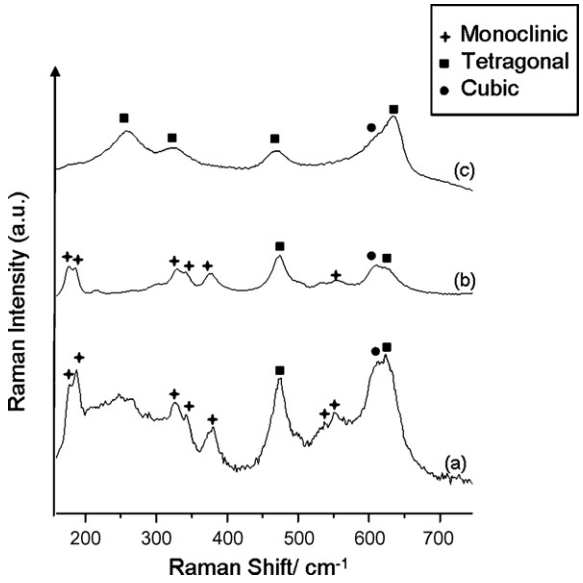

Fig. 6. FT Raman spectra of the as-prepared $HS_{II,st}$ sample (a) and the same powder calcined at 600 (b) and 700 °C (c).

150 °C is accompanied by two endothermic peaks centred at 100 and 145 °C and can correspond among other phenomena to the desorption of physically adsorbed water.[42] There must be taken into account that the powder was not washed after the synthesis and the Cl^- ions, from both the zirconium and yttrium chlorides, together with the NH_4^+ ions can form ammonium chloride. This salt presents an endothermic peak at 188 °C that indicates the change of its crystal structure. Above 200 °C, the substance sublimes and after sublimation it dissociates completely in the gaseous phase into ammonia and hydrochloric acid.[43,44] Hence, the weight loss (37 wt.%) associated to an endothermic peak centred at 220 °C can be assigned to the above mentioned processes.

Finally, a broad exothermic peak appears from 420 to 1000 °C and can be due to different events that can occur at the same time such as the oxidation of residual organics, the crystallization of ZrO_2 from the unreacted fraction of $ZrOCl_2$,[14] and zirconia phase transformations that could be take place between 600 and 700 °C.

The FT-Raman spectra for the as-prepared $HS_{II,st}$ sample and the same powder calcined at 600 and 700 °C are shown in Fig. 6. The corresponding FT-Raman spectra of the as-prepared powders and the powders calcined at 600 °C are very similar, however, for the powder calcined at 700 °C the bands at 178, 186, 530 and 552 cm^{-1} corresponding to the monoclinic phase disappear.[40] At the same time, the bands at 255 and 320 cm^{-1} related to the tetragonal phase appear.[41] This fact confirms that one of the processes registered between 600 and 700 °C by means of the DTA and associated to the broad exothermic peak could correspond to the monoclinic–tetragonal zirconia phase transition.

In summary, under the hydrothermal conditions described, urea should be added to accelerate the reagent hydrolysis reaction avoiding the formation of monoclinic and tetragonal phases as secondary phases (detected by XRD). It is established that under dilute conditions an excess of urea is needed to reach a basic pH, achieving the total hydroxylation/condensation during the hydrothermal synthesis to obtain YSZ as major phase. A thermal treatment that includes two steps (80 °C/72 h and 180 °C/72 h) is needed to force the hydrolysis of the urea at 80 °C and then the crystallization of the powders at 180 °C.

Table 3
Morphological and crystallographic characteristics of the $HS_{II,sup}$, and $HS_{II,st}$ as-prepared powders dried at 60 °C.

Powder	Crystallographic phases[a]	d_{BET} (nm)	d_v50 (nm)	F_{ag}
$HS_{II,sup}$	c, m↓	9	300	33
$HS_{II,st}$	c, t↓, m↓	10	300	31

↓ means that the phase is not detected by XRD but by FT-Raman.
[a] m, t and c are monoclinic, tetragonal and cubic phases, respectively.

3.2. Dispersion study of the synthesized nanoparticles

In this study, two different synthesis, $HS_{II,st}$ and $HS_{II,sup}$ which reach different pHs at the end of the reaction, i.e. 3.3 and 9.7, respectively, are considered in order to investigate the urea behaviour as dispersant in different post-reaction media. In a first approach, the precipitated powders were mechanically stirred and suspended in their own synthesis mother liquor.

The data summarized in Table 3 include the morphological characterization, the crystallographic phases identified in the as-prepared powders for $HS_{II,sup}$ and $HS_{II,st}$, the primary particle size (d_{BET}), average particle size (d_v50) and the agglomeration factor (F_{ag}). The specific surface area measurement of the samples dried at 60 °C, are in the range of 160–190 $m^2\ g^{-1}$ (Table 2). Considering the measured density and assuming spherical morphology, the BET diameter[36] (d_{BET}) of particles is between 8 and 10 nm. The calculated BET diameter is in accordance with the data reported in the literature[19] for YSZ nanoparticles and consistent with the observed primary particle size, lower than 10 nm observed in TEM micrographs (Fig. 3), and typical of powders obtained by this synthesis method.[45]

According to previous works[46–48] urea precipitation was thought to be very effective in making weakly agglomerated ultrafine powders via the homogeneous hydrolysis of cations under a pH yielded by a fixed concentration of urea. The F_{ag} is high in both cases, which indicates quite agglomerated nanoparticles, as is expected when water is used as solvent in the hydrothermal synthesis.[49] Average particle sizes measured are also shown in Table 3. The particles show a high size in both cases, reaching an average diameter of 300 nm, being higher than that of the agglomerate powder shown in the micrographs obtained by TEM (Fig. 3).

The pH of the mother liquor after the hydrothermal synthesis depends on the urea amount used as starting reagent (Table 2). As is explained above, when the urea was added in quantities higher than the stoichiometry, the pH at the end of the reaction was alkaline (9.7), however, when the quantity added was stoichiometry the final pH resulted acidic (3.3). The particles suspended in the mother liquor by mechanical stirring for 1 h, have a positive or negative charge on their surfaces depending

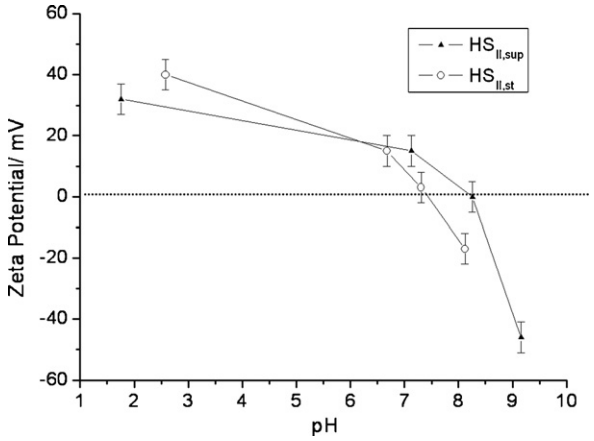

Fig. 7. Zeta potential vs. pH for the as-synthesized $HS_{II,sup}$, $HS_{II,st}$ powders.

on the pH of the suspension. That means that the powders prepared from the superstoichiometry amount of urea are negatively charged on their surface, while those particles obtained by $HS_{II,st}$ synthesis are positively charged. The surface evolution in terms of zeta potential vs. the pH of both suspensions is plotted in Fig. 7.

The isoelectric point (IEP) (Fig. 7) of the $HS_{II,st}$ suspension is close to 7.5, however, the IEP of the $HS_{II,sup}$ powder suspension is ≈8.2. The shift of the IEP value is too large to be attributed to the presence of different phases in both powders.[50–51] In fact, the IEP of synthetic and commercial YSZ and Y-TZP powders reported in the literature are in the range of pH 5.5–7.5.[12,51] Hence, the IEP shift up of the $HS_{II,sup}$ suspension can be attributed to the adsorption of charged species dissolved in the mother liquor. As is mentioned above that adsorption was confirmed by the DTA-TG curves (Fig. 5) and by the FTIR spectra carried out on the as-synthesized $HS_{II,sup}$ and $HS_{II,st}$ powders (not shown here).

Fig. 8a shows the dispersion degree achieved by the particles in the $HS_{II,sup}$, $HS_{II,st}$ suspensions when sonication was applied for different times.

As is well known, urea is used as dispersing agent for nanoparticles.[19,20] In this study, a new suspension ($HS_{II,st}$ + U) was prepared for comparative purposes, where the urea amount needed (U) to fit the ZrO^{+2}: urea molar ratio used at the superstoichiometric synthesis (67 wt.% on dry solid basis) was added to the $HS_{II,st}$ suspension in the post-synthesis medium. The particle size distribution was measured after sonication was applied. The suspension is maintained at the pH achieved after synthesis, as is indicated in the legend on Fig. 8. For the suspension $HS_{II,st}$ + U, the natural pH of $HS_{II,st}$ is kept constant after the urea addition as dispersant agent since the urea is a weak base.[12] The three slurries showed the same behaviour when different ultrasonication times were applied. The average particle size of the agglomerates decreases as sonication time increases up to

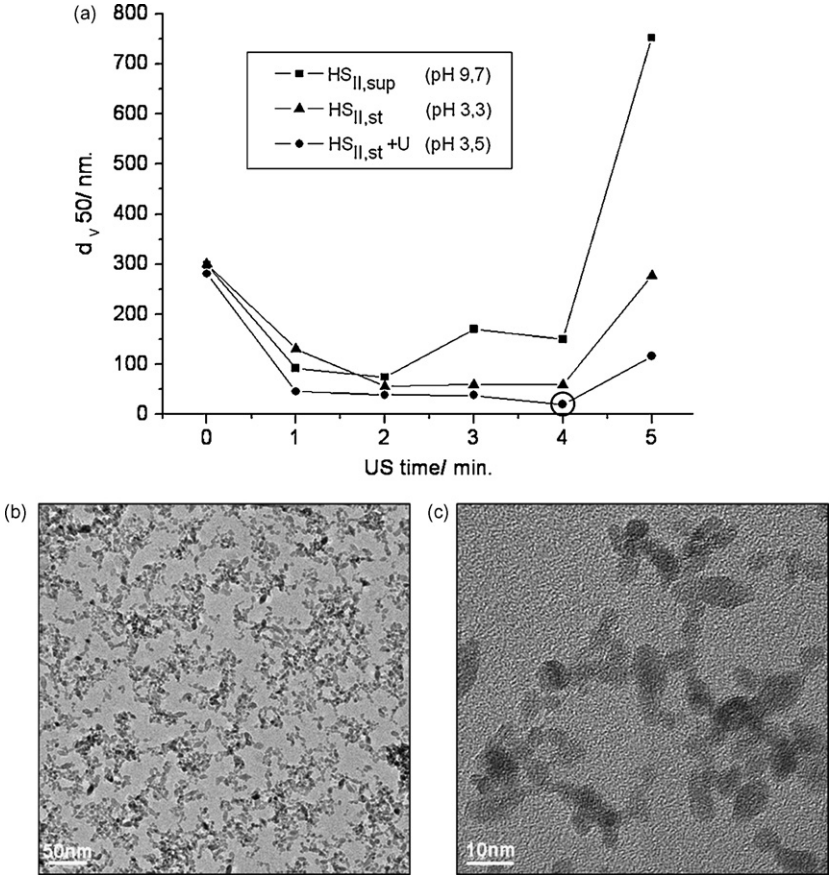

Fig. 8. Average particle size vs. sonication time for $HS_{II,sup}$, $HS_{II,st}$ and $HS_{II,st}$ + U samples. For the latest case ($HS_{II,st}$ + U sample after 4 min of US) HR-TEM micrographs, that corresponds to the point surrounded by a circle [Fig. 8(a)], are shown.

Table 4
The cation/anion relative sizes and the average particle size (d_v50) of nanoparticles obtained after the $HS_{II,sup}$, $HS_{II,st}$ and $HS_{II,st}$ + U hydrothermal synthesis followed by 2, 3 and 4 min sonication times, respectively.

	$HS_{II,sup}$		$HS_{II,st}$		$HS_{II,st}$ + U
d_v50 (nm)	75	<	55	<	20
Anion/cation relative sizes	Cl^-	<	NH_4^+	<	$[(H_2N)_2COH]^+$

2 min in the case of $HS_{II,sup}$ and $HS_{II,st}$ suspensions, and 4 min in the $HS_{II,st}$ + U. The minimum values of the average particle size achieved were 75 and 55 nm for $HS_{II,sup}$ and $HS_{II,st}$ powders respectively, and 20 nm for $HS_{II,st}$ + U powders. The latest can be observed in the HR-TEM micrographs shown in Fig. 8. The picture with the highest magnification shows particles with a size even less than ~5 nm. This result indicates that the d_{BET} determined from the nitrogen adsorption isotherm data[35,36] gives an overestimated primary particle size due to the growth/aggregation/agglomeration effect during synthesis or/and drying processes. In addition, when the above mentioned sonication times are exceeded, reagglomeration is produced and highest average particle sizes are observed by DLS. In all cases, the results show that the agglomerates are weak since they are easily broken with a low energy supplied by the sonication probe.

For the $HS_{II,st}$ and $HS_{II,st}$ + U suspensions, as mentioned above the pH_f is acid in both cases, reaching an average particle size lower than that of $HS_{II,sup}$ powders having the latest a basic pH. That could indicate that the deagglomeration is more effective at acid pH (3.3–3.5). In particular, when the urea was added after the $HS_{II,st}$ synthesis seems to provoke the most effective deagglomeration. In fact, the F_{ag} calculated (d_v50/d_{BET}) for $HS_{II,st}$ + U suspension after 4 min US was 2, being reduced a 93% if we compare with the F_{ag} value for the as-prepared $HS_{II,st}$ suspension (Table 3). It is noticed that, in both synthesis ($HS_{II,sup}$ and $HS_{II,st}$), the most of initial urea content was hydrolyzed at the end of the synthesis (Eq. (1)). It has been proved that the reaction yield of the synthesis was close to 90 wt.%, thus unreacted urea could still remain in the mother liquor after the hydrothermal synthesis. Considering Eqs. (1) and (4), the predominant dissolved and negatively charged specie after the synthesis at basic pH can be the Cl^- ions that, mainly maintained anchored to the particles surface.[50] However, under acidic conditions dissolved species in the mother liquor can be the NH_4^+ ions, coming from the urea hydrolyzation (Eq. (1)), and $[(H_2N)_2COH]^+$ from the protonation of urea in water at acid pH.[52] Those species can effectively contribute to the defloculation of the nanoparticles obtained after the synthesis and a subsequent sonication dispersion since both NH_4^+ and $[(H_2N)_2COH]^+$ have an oxidation state of 1^+ and are big cations, although $[(H_2N)_2COH]^+$ is higher than NH_4^+.[53] Hence, there is a direct correlation between the ion size and the value of the mean particle size (d_v50) achieved after the sonication, as is shown in Table 4, verifying the dispersion improvement when urea is added after de synthesis.

The dispersion effect of the extra-amount of urea added as deflocculant has been evaluated at different pH values, by measuring the zeta potential of the $HS_{II,st}$ + U suspension after 4 min of US and without sonication treatment (Fig. 9). The zeta

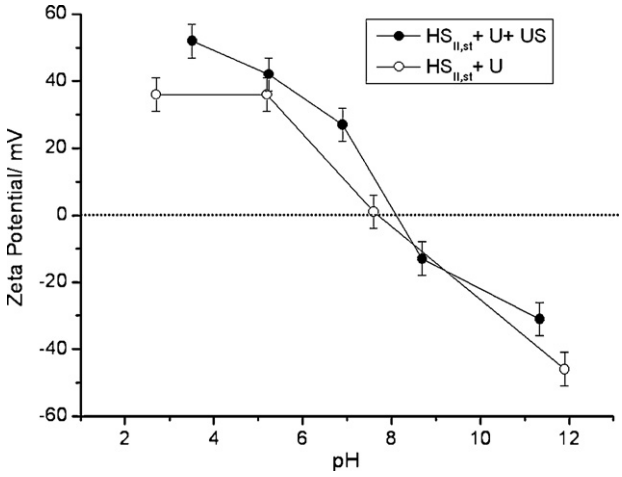

Fig. 9. Zeta potential curves of the $HS_{II,st}$ + U suspension after 4 min of US ($HS_{II,st}$ + U + US) and without ($HS_{II,st}$ + U) sonication.

potential curve determined for $HS_{II,st}$ + U suspension before sonication is similar to that obtained for $HS_{II,st}$, being the IEP close to 7.5. When sonication was applied, the IEP shifts up to pH 8.1, and the zeta potential values increased for acid pH values. The agglomerates break down after sonication gives rise to the urea adsorption on the new created surfaces. Hence, the urea adsorption promotes the shift up of the IEP. The urea is protonated at acid pH $[(H_2N)_2COH]^+$ enhancing the electrostatic repulsive interaction between nanoparticles[52] and, shifting the zeta potential curve. Hence, the specific adsorption of the urea on the particle surface promotes the development of effective electrosteric forces acting between particles contributing to keep an elevated degree of deflocculation in the suspension at acid pH, as shown in Fig. 8. Consequently, the urea positively charged acts as a polyelectrolyte that could be adsorbed on the particle surface, improving the particles stabilization by means of a combination of both, electrostatic and steric mechanisms.[53]

To optimize the urea content needed to assure the obtention of deflocculated YSZ nanoparticles in the mother liquor during the synthesis, the zeta potential evolution of the $HS_{II,st}$ suspensions with different urea additions after the synthesis was determined.

Fig. 10a shows the zeta potential measurements vs. the urea concentration for $HS_{II,\ st}$ suspension. All the suspensions were sonicated for 4 min before the zeta potential determination. The $HS_{II,st}$ suspension achieved the maximum zeta potential value when 0.5 wt.% urea is added, indicating that this is the most suitable urea quantity which should be added in order to achieve the highest particle stability under those conditions. The plot in Fig. 10b shows the corresponding size distributions obtained when the different quantities of urea are tested. The best distribution corresponds to the suspension with a 0.5 wt.% urea addition since a monomodal curve is obtained indicating the lowest average particle size being 24 nm. These results demonstrate that it is not necessary the addition of a large amount of urea that is usually added,[19,20] neither as reagent nor as dispersant, to obtain dispersed nanoparticles through a hydrothermal synthesis process under mild conditions.

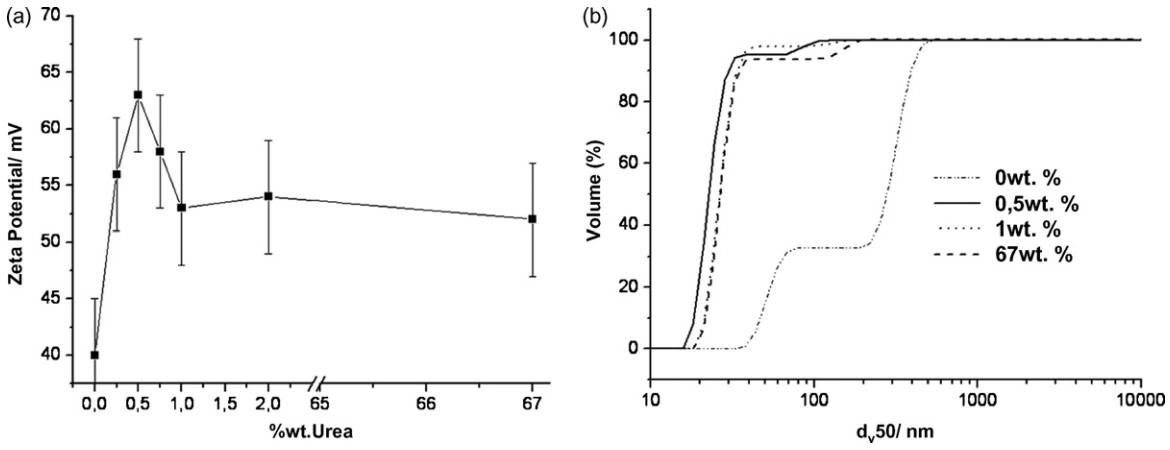

Fig. 10. (a) Zeta potential vs. urea concentration for the as-synthesized $HS_{II,\ st}$ and (b) their corresponding distribution size for the different urea additions.

Otherwise, urea should be added as dispersant agent at the end of the reaction, being more effective in acid media. In this way urea is protonated and allows us to obtain small agglomerates (average particle size of $d_v50 = 20$ nm). That value is very close to the primary particle size ($d_{BET} \leq 10$ nm) achieved by ultrasound sonication and measured by DLS. In addition, this study establishes that the protonated urea allows us to reach the maximum values of the zeta potential for the YSZ nanoparticles, i.e. >30 mV at acid pH. In summary, urea as dispersant works better when is added at the end of the reaction, i.e. in the post-reaction medium, than when the excess of the unreacted urea is expected to be used for such purpose.

4. Conclusions

It has been established that under dilute conditions an adequate amount of urea for both, the synthesis and the dispersion powder in the post-reaction medium is needed. Urea addition as synthesis reagent is required to maintain the pH > 5 during the synthesis process in order to avoid the Y^{3+} dissolution in the mother liquor and to obtain YSZ as major phase. Urea addition as dispersant should be performed after the synthesis process keeping the pH between 5 and 7 to promote an effective dispersion. At those pHs the urea is protonated and acts as a polyelectrolyte that could be able to adsorb on the particle surface. Under those conditions, the measured average particle size for the synthesized YSZ is ~20 nm and the agglomeration factor is 2. However, by HR-TEM particles of the suspension dispersed in the post-reaction medium with a size even less than 5 nm can be observed. Hence, the particle size of the as-synthesized powders is lower than the value of the primary particle size estimated by BET (8–10 nm).

Acknowledgements

This work has been supported by CICYT (Spain, contract MAT2006-01038) projects. I. Gonzalo-Juan acknowledges the Spanish Ministry of Science and Innovation for the concession of a FPU-AP2006 grant. The authors wish to thank Prof. Dr. C. Domingo and Dr. F. Rubio for useful discussions in FT-Raman studies.

References

1. Politova, T. I. and Irvine, J. T. S., Investigation of scandia-yttria-zirconia system as an electrolyte material for intermediate temperature fuel cells-influence of yttria content in the system $(Y_2O_3)_x(Sc_2O_3)_{11-x}(ZrO_2)_{89}$. *Solid State Ionics*, 2004, **168**(1–2), 153–165.
2. Guan, J., Doshi, R., Lear, G., Montgomery, K., Ong, E. and Minh, N., Ceramic oxygen generators with thin-film zirconia electrolytes. *J. Am. Ceram. Soc.*, 2002, **85**(11), 2651–2654.
3. Minh, N. Q., Ceramic fuel-cell. *J. Am. Ceram. Soc.*, 1993, **76**, 563–588.
4. Weber, A. and Ivers-Tiffee, E., Materials and concepts for solid oxide fuel cells (SOFCs) in stationary and mobile applications. *J. Power Sources*, 2004, **127**, 273–283.
5. Li, Y., Xie, Y., Gong, J., Chen, Y. and Zhang, Z., Preparation of Ni/YSZ materials for SOFC anodes by buffer-solution method. *Mater. Sci. Eng. B*, 2001, **86**, 119–122.
6. Cushing, B. L., Kolesnichenko, V. L. and O'Connor, C. J., Recent advances in the liquid-phase syntheses of inorganic nanoparticles. *Chem. Rev.*, 2004, **104**(9), 3893–3946.
7. Masala, O. and Seshadri, R., Synthesis routes for large volumes of nanoparticles. *Annu. Rev. Mater. Res.*, 2004, **34**, 41–81.
8. Tsukada, T., Venigalla, S., Morrone, A. A. and Adair, J. H., Low-temperature hydrothermal synthesis of yttrium-doped zirconia powders. *J. Am. Ceram. Soc.*, 1999, **82**(5), 1169–1174.
9. Matsui, K. and Ohgai, M., Formation mechanism of hydrous zirconia particles produced by the hydrolysis of $ZrOCl_2$ solutions: III, Kinetics study for the nucleation and crystal-growth processes of primary particles. *J. Am. Ceram. Soc.*, 2001, **84**(10), 2303–2312.
10. Demazeau, G. J., Solvothermal processes: a route to the stabilization of new materials. *Mater. Chem.*, 1999, **9**, 15–18.
11. Byrappa, K. and Adschiri, T., Hydrothermal technology for nanotechnology. *Prog. Cryst. Growth Charact. Mater.*, 2007, **53**(2), 117–166.
12. Hu, M. Z. C., Harris, M. T. and Byers, C. H., Nucleation and growth for synthesis of nanometric zirconia particles by forced hydrolysis. *J. Colloid Interface Sci.*, 1998, **198**(1), 87–99.
13. Dell'Agli, G. and Mascolo, G., Hydrothermal synthesis of ZrO_2-Y_2O_3 solid solutions at low temperature. *J. Eur. Ceram. Soc.*, 2000, **20**(2), 139–145.
14. Dell'Agli, G. and Mascolo, G., Zirconia-yttria (8 mol%) powders hydrothermally synthesized from different Y-based precursors. *J. Eur. Ceram. Soc.*, 2004, **24**(6), 915–918.
15. Dell'Agli, G., Mascolo, G., Mascolo, M. C. and Pagliuca, C., Weakly-agglomerated nanocrystalline $(ZrO_2)_{0.9}(Yb_2O_3)_{0.1}$ powders hydrother-

mally synthesized at low temperature. *Solid State Sci.*, 2006, **8**(9), 1046–1050.
16. Cabanas, A., Darr, J. A., Lester, E. and Poliakoff, M., Continuous hydrothermal synthesis of inorganic materials in a nearcritical water flow reactor; the one-step synthesis of nano-particulate $Ce_{1-x}Zr_xO_2$ (x = 0–1) solid solutions. *J. Mater. Chem.*, 2001, **11**(2), 561–568.
17. Hakuta, Y., Ohashi, T., Hayashi, H. and Arai, K., Hydrothermal synthesis of zirconia nanocrystals in supercritical water. *J. Mater. Res.*, 2004, **19**(8), 2230–2234.
18. Rao, B. V. N. and Schreiber, T. P., Scanning-transmission electron-microscope analysis of solute partitioning in a partially stabilized zirconia. *J. Am. Ceram. Soc.*, 1982, **65**(3), C44–C45.
19. Zhang, Y. W., Sun, X., Xu, G., Tian, S. J., Liao, C. S. and Yan, C. H., Co-doping effects of Y^{3+} and Sc^{3+} on the crystal structures, nanoparticle properties and electrical behavior of ZrO_2 solid solutions prepared by a mild urea-based hydrothermal method. *Phys. Chem. Chem. Phys.*, 2003, **5**(10), 2129–2134.
20. Xu, G., Zhang, Y. W., Liao, C. S. and Yan, C. H., Hydrothermal synthesis of weakly agglomerated nanocrystalline scandia-stabilized zirconia. *J. Am. Ceram. Soc.*, 2002, **85**(4), 995–997.
21. Vasylkiv, O. and Sakka, Y., Synthesis and colloidal processing of zirconia nanopowder. *J. Am. Ceram. Soc.*, 2001, **84**(11), 2489–2494.
22. Vasylkiv, O., Sakka, Y. and Skorokhod, V. V., Features of preparing nano-size powders of tetragonal zirconium dioxide stabilized with yttrium. *Powder Metall. Met. C*, 2005, **44**(5–6), 228–239.
23. Xin, X. S., Lu, Z., Huang, X. Q., Sha, X. Q., Zhang, Y. H. and Su, W. H., Influence of synthesis routes on the performance from weakly agglomerated yttria-stabilized zirconia nanomaterials. *Mater. Res. Bull.*, 2006, **41**(7), 1319–1329.
24. Yoshimura, M. and Somiya, S., Hydrothermal synthesis of crystallized nanoparticles of rare earth-doped zirconia and hafnia. *Mater. Chem. Phys.*, 1999, **61**(1), 1–8.
25. Lin, J. D. and Duh, J. G., Coprecipitation and hydrothermal synthesis of ultrafine 5.5 mol% CeO_2-2 mol% YO1.5-ZrO_2 powders. *J. Am. Ceram. Soc.*, 1997, **80**(1), 92–98.
26. Lin, J. D. and Duh, J. G., Crystallite size and microstrain of thermally aged low-ceria- and low-yttria-doped zirconia. *J. Am. Ceram. Soc.*, 1998, **81**(4), 853–860.
27. Zhang, Y. W., Xu, G., Yan, Z. G., Yang, Y., Liao, C. S. and Yan, C. H., Nanocrystalline rare earth stabilized zirconia: solvothermal synthesis via heterogeneous nucleation-growth mechanism, and electrical properties. *J. Mater. Sci.*, 2002, **12**(4), 970–977.
28. Hirano, M. and Morikawa, H., Hydrothermal synthesis and phase stability of new zircon- and scheelite-type ZrGeO4. *Chem. Mater.*, 2003, **15**(13), 2561–2566.
29. Si, R., Zhang, Y. W., Li, S. J., Lin, B. X. and Yan, C. H., Urea-based hydrothermally derived homogeneous nanostructured Ce1-xZrxO2 (x = 0–0.8) solid solutions: a strong correlation between oxygen storage capacity and lattice strain. *J. Phys. Chem. B*, 2004, **108**(33), 12481–12488.
30. Xu, G., Zhang, Y. W., Liao, C. S. and Yan, C. H., Grain size-dependent electrical conductivity in scandia-stabilized zirconia prepared by a mild urea-based hydrothermal method. *Solid State Ionics*, 2004, **166**(3–4), 391–396.
31. Xu, G., Zhang, Y. W., Liao, C. S. and Yan, C. H., Doping and grain size effects in nanocrystalline ZrO_2–Sc_2O_3 system with complex phase transitions: XRD and Raman studies. *Phys. Chem. Chem. Phys.*, 2004, **6**(23), 5410–5418.
32. Xu, G., Zhang, Y. W., Liao, C. S. and Yan, C. H., Tetragonal-to-monoclinic phase transitions in nanocrystalline rare-earth-stabilized zirconia prepared by a mild hydrothermal method. *J. Am. Ceram. Soc.*, 2004, **87**(12), 2275–2281.
33. Zhang, Y. W., Sun, X., Xu, G. and Yan, C. H., Doping effects of Yb^{3+} on the crystal structures, nanoparticle properties and electrical behaviors of ZrO_2 derived from a facile urea-based hydrothermal route. *Solid State Sci.*, 2004, **6**(6), 523–531.
34. Si, R., Zhang, Y. W., Wang, L. M., Li, S. J., Lin, B. X., Chu, W. S. *et al.*, Enhanced thermal stability and oxygen storage capacity for $Ce_xZr_{1-x}O_2$ ((x) = 0.4–0.6) solid solutions by hydrothermally homogenous doping of trivalent rare earths. *J. Phys. Chem. C*, 2007, **111**(2), 787–794.
35. Gregg, S. J. and Sing, K. S., *Adsorption, Surface Area and Porosity*. Academic Press, London, UK, 1992.
36. German, R. M., A measure of the number of particles in agglomerates. *Int. J. Powder Metall.*, 1996, **32**(4), 365–373.
37. Harper, C. A., *Handbook of Ceramics, Glasses and Diamonds*. McGraw-Hill companies, Inc., USA, 2001.
38. Fariñas, J. C., Moreno, R., Requena, J. and Moya, J. S., Acid basic stability of Y-TZP ceramics. *Mater. Sci. Eng. A*, 1989, **109**, 97–99.
39. Hirata, T., Asari, E. and Kitajima, M., Infrared and raman-spectroscopic studies of ZrO_2 polymorphs doped with Y_2O_3 or CeO_2. *J. Solid State Chem.*, 1994, **110**, 201–207.
40. Li, Q., Xia, T., Liu, X. D., Ma, X. F., Meng, J. and Cao, X. Q., Fast densification and electrical conductivity of yttria-stabilized zirconia nanoceramics. *Mater. Sci. Eng. B*, 2007, **138**(1), 78–83.
41. Mori, M., Hiei, Y., Itoh, H., Tompsett, G. A. and Sammes, N. M., Evaluation of Ni and Ti-doped Y_2O_3 stabilized ZrO_2 cermet as an anode in high-temperature solid oxide fuel cells. *Solid State Ionics*, 2003, **160**(1–2), 1–14.
42. Hua, Z. L., Wang, X. M., Xiao, P. and Shi, J. L., Solvent effect on microstructure of yttria-stabilized zirconia (YSZ) particles in solvothermal synthesis. *J. Eur. Ceram. Soc.*, 2006, **26**(12), 2257–2264.
43. Erdey, L., Gal, S. and Liptay, G., Thermoanalytical properties of grade reagents. Ammonium salts. *Talanta*, 1964, **11**, 913–940.
44. Olszak-Humienik, M., On the thermal stability of some ammonium salts. *Thermochim. Acta*, 2001, **378**, 107–112.
45. Staiger, M., Bowen, P., Ketterer, J. and Bohonek, J., Particle size distribution measurement and assessment of agglomeration of commercial nanosized ceramic particles. *J. Dispersion Sci. Technol.*, 2002, **23**(5), 619–630.
46. Huang, Y. X. and Guo, C. J., Synthesis of nanosized zirconia particles via urea hydrolysis. *Powder Technol.*, 1992, **72**(2), 101–104.
47. Hirano, M. and Inagaki, M., Preparation of monodispersed cerium(IV) oxide particles by thermal hydrolysis: influence of the presence of urea and Gd doping on their morphology and growth. *J. Mater. Chem.*, 2000, **10**(2), 473–477.
48. Cote, L. J., Teja, A. S., Wilkinson, A. P. and Zhang, Z. J., Continuous hydrothermal synthesis and crystallization of magnetic oxide nanoparticles. *J. Mater. Res.*, 2002, **17**(9), 2410–2416.
49. Wang, X. M., Lorimer, G. and Xiao, P., Solvothermal synthesis and processing of yttria-stabilized zirconia nanopowder. *J. Am. Ceram. Soc.*, 2005, **88**(4), 809–816.
50. Tallon, C., Moreno, R. and Nieto, M. I., Synthesis of ZrO_2 nanoparticles by freeze drying. *Int. J. Appl. Ceram. Technol.*, 2008, doi:10.111/;.1744-7402.2008.02279.X.
51. López-López, E., Baudín, C. and Moreno, R., Synthesis of zirconium titanate-based materials by colloidal filtration and reaction sintering. *Int. J. Appl. Ceram. Technol.*, 2008, **5**, 394–400.
52. Morrison, R. T., *Organic Chemistry*, ed. Prentice Hall International (UK) Limited, London, 1992, ISBN 0-13-643669-2.
53. Moreno, R., The role of slip additives in tape casting technology: part I—solvents and dispersants. *Am. Ceram. Soc. Bull.*, 1992, **71**, 1521–1530.